Temperature relaxation in dense plasmas

Gérald Faussurier* and Christophe Blancard
CEA, DAM, DIF, F-91297 Arpajon, France

(Received 9 October 2015; revised manuscript received 22 January 2016; published 18 February 2016)

We present a model to calculate temperature-relaxation rates in dense plasmas. The electron-ion interaction potential and the thermodynamic data of interest are provided by an average-atom model. This approach allows the study of the temperature relaxation in a two-temperature electron-ion system.

DOI: 10.1103/PhysRevE.93.023204

I. INTRODUCTION

In inertial confinement fusion (ICF), the ions of the high-temperature plasma undergo fusion reactions to produce α particles. These particles exchange their energy with the electrons and the ions of the surrounding environment but at different rates due to the mass difference between electrons and ions. This causes a difference between electron and ion temperatures that drives energy exchange between the two subsystems in order to reach an equilibration temperature. This electron-ion temperature relaxation is one of the key processes that should be described with care in order to capture the ignition phenomenon of a thermonuclear plasma [1–3]. This task is challenging due to the complex physical regimes encountered in which quantum and correlation effects come to play. These physical regimes span the warm dense matter or high energy density physics regimes.

Since the seminal works of Landau [4] and Spitzer [5] on classical and weakly coupled plasmas, various developments can be found in the literature to study the temperature relaxation in dense plasmas [6–32]. When people attempt to calculate the temperature-relaxation rates, they usually assume that the electrons and ions interact weakly. This allows that each subsystem can be described by a temperature T_e for the electrons and T_i for the ions. In the parameter-free calculations, mixtures are usually avoided.

In this paper, we propose to use the model of Daligault and Dimonte [23] to calculate the electron-ion temperature-relaxation rates in dense plasmas including self-consistently the effects of screening and electron degeneracy but neglecting correlations between electrons and ions. The average-atom model SCAALP [33,34] is used to calculate the electron-ion interaction potential and the average ionization. The original model SCAALP has been modified to take into account the fact that $T_e \neq T_i$. Comparisons with molecular dynamics simulations are done to test the accuracy of the relaxation rates. The paper is organized as follows. The model is presented in a theoretical part. Then, numerical calculations are shown for dense hydrogen and carbon plasmas. The role of ionization is outlined as well as the thermodynamic state at equilibration. The last part is the conclusion.

II. THEORY

A. SCAALP model

The SCAALP model [33,34] is based on a variational approach to describe the thermodynamic and transport properties of warm and hot dense matter in local thermodynamic equilibrium. The electronic and ionic structures are determined self-consistently using an average-atom approach based on the finite-temperature density-functional theory and the Gibbs-Bogolyubov inequality. In the SCAALP model, the plasma is viewed as an effective medium of neutral pseudoatoms (NPAs) interacting via an interatomic potential $\Phi_{eff}(r)$. Electrons of the NPA satisfy a Schrödinger equation with a central symmetric potential $V_{eff}(r)$. These two effective potentials are determined by the electronic structure and ionic distribution of the plasma. Polarization, exchange, and correlation effects are taken into account within both $V_{eff}(r)$ and $\Phi_{eff}(r)$. We use a finite-temperature exchange and correlation functional [35]. We can describe the ionic subsystem using either the hard-sphere (HS) system or an effective one-component plasma (OCP) [36]. In both cases, the effective parameter of the ionic subsystem is derived from the Gibbs-Bogolyubov inequality. The best electron density $n(r)$ of the NPA is also found using the Gibbs-Bogolyubov inequality, leading to a tractable expression for $V_{eff}(r)$ from which $n(r)$ is calculated [37]. The chemical potential μ is determined such that

$$\int_0^{R_{WS}} 4\pi r^2 n(r) dr = Z, \tag{1}$$

where Z is the nuclear charge of the element and R_{WS} is the Wigner-Seitz radius. R_{WS} is related to the ion density N_i through the equation $4\pi R_{WS}^3 N_i/3 = 1$. The average ionization $\bar{Z}$ is calculated [38] by the formula $\bar{Z} = n(R_{WS})/N_i$, from which one can deduce the electron density $N_e = \bar{Z} N_i$. The free energy F_{tot} of the ion and electron system is minimized with respect to the electron density and the effective parameter of the ionic subsystem. By construction, the SCAALP model is thermodynamically consistent. One can calculate equation of state data from the free energy [39] as well as various electron and ion transport coefficients and stopping power [34], opacity [40], or x-ray Thomson scattering spectra [37,41]. This model is strictly speaking limited to the case for which $T_e = T_i$. We have modified the SCAALP model to describe situations in which the electron and ion temperatures are different. We choose to describe the ionic environment with an OCP system with a plasma coupling parameter such that

$$\Gamma_{ii} = \frac{\bar{Z}^2 e^2}{R_{WS} k_B T_i}, \tag{2}$$

where e is the elementary charge and k_B is the Boltzmann constant. There are still two loops to solve the SCAALP equations, i.e., an external one on the Γ_{ii} parameter that describes the ionic structure and an internal one on the

*Corresponding author: gerald.faussurier@cea.fr

electronic structure. The system of equations when $T_e \neq T_i$ converges well. When the convergence is achieved, one has data from the SCAALP model such as the average ionization $\bar{Z}$ or the electron-ion interaction-potential $V_{ei}(r)$ that depend both on T_e and T_i. $V_{ei}(r)$ is different from $V_{eff}(r)$ since this potential depends explicitly on the pair correlation function but not $V_{ei}(r)$ which is related to one NPA. This is an approximate but powerful way to describe a two-temperature electron-ion system. To be explicit [37,42], for $r \leqslant R_{WS}$,

$$V_{ei}(r) = -\frac{Ze^2}{r} + V_{dir}(r) + V_{xc}[n(r)] - V_{xc}[n(R_{WS})], \quad (3)$$

where $V_{xc}(r)$ is the exchange-correlation potential and $V_{dir}(r)$ is the direct potential that satisfies the Poisson equation

$$\nabla^2 V_{dir} = -4\pi e^2 n(r). \quad (4)$$

For $r > R_{WS}$, $V_{ei}(r) = 0$. $V_{eff}(r)$ is calculated as follows, i.e.,

$$V_{eff}(\mathbf{r}) = V_{ei}(\mathbf{r}) + N_i \int V_{ei}(\mathbf{r}-\mathbf{r}')h_{OCP}(\mathbf{r}',\Gamma_{ii})d\mathbf{r}' \quad (5)$$

where $h_{OCP}(\mathbf{r},\Gamma_{ii})$ is the OCP pair correlation function related to the pair distribution $g_{OCP}(\mathbf{r},\Gamma_{ii})$ by the identity $g_{OCP}(\mathbf{r},\Gamma_{ii}) = h_{OCP}(\mathbf{r},\Gamma_{ii}) + 1$. We have included the correlation effects since only the exchange terms appear in the original Hartree-Fock formalism [33,34]. For simplicity and numerical reasons, exchange and correlation effects are calculated using the density functional theory in the local density approximation. One can see that the spherically symmetric effective potential $V_{eff}(r)$ is the sum of two contributions, i.e., the NPA potential $V_{ei}(r)$ and the effect of environment $N_i \int V_{ei}(\mathbf{r}-\mathbf{r}')h_{OCP}(\mathbf{r}',\Gamma_{ii})d\mathbf{r}'$. When we have complete disorder, the pair distribution function is equal to 1 so the pair correlation function is equal to zero and $V_{eff}(r) = V_{ei}(r)$. We recover the usual average-atom model [37,42]. The environment term can induce not-trivial dense-plasma effects on the electronic structure of the average-atom model. The NPA electron density $n(\mathbf{r})$ is calculated as follows, i.e.:

$$n(\mathbf{r}) = \sum_n \frac{|\varphi_n(\mathbf{r})|^2}{1 + e^{\beta_e(\varepsilon_n - \mu)}}, \quad (6)$$

where the bound and free one-electron wave functions satisfy the Schrödinger equation

$$\left[-\frac{\hbar^2\nabla^2}{2m_e} + V_{eff}(\mathbf{r})\right]\varphi_n(\mathbf{r}) = \varepsilon_n\varphi_n(\mathbf{r}). \quad (7)$$

$\beta_e = 1/k_B T_e$, m_e is the electron mass, and $\hbar$ is the reduced Planck constant. One can see that the electron density depends on T_e but also on T_i through the environment term in $V_{eff}(r)$. This explains why $V_{ei}(r)$ or $\bar{Z}$ depend on both T_e and T_i. We insist on the fact that we do not need any free energy nor GBI in the present approach. The SCAALP model contains no adjustable parameters. The input parameters of the calculation are nuclear charge of the element, the mass density, and the electron and ion temperatures when we take into account the fact that T_e can be different from T_i. Note that we have not developed a self-consistent treatment of a system with two different temperatures from first principles. Instead of using the SCAALP model with a fixed Γ_{ii}, we write this parameter as in Eq. (2) and perform calculations at fixed T_i. Since $\bar{Z}$ must be determined self-consistently, we have two loops instead of simply one loop on the electronic structure when we perform calculations at fixed Γ_{ii} to describe $T_e \neq T_i$ systems. The treatment of $T_e \neq T_i$ from first principles is a difficult topic that deserves a particular study [43]. Finally, using an OCP as in Eq. (2) to describe the ionic structure and combining it with the NPA approach is clearly an approximation. It is an option in the SCAALP model because the Gibbs-Bogolyubov inequality is very robust, contrary to the (VM)HNC option [34] that does not always converge. We use the HS and the OCP systems because one has access relatively easily to the excess free energy and to the pair distribution from one parameter, i.e., the HS packing fraction or the plasma coupling parameter. In standard calculations, we prefer to use the HS system that is more closely related to the notion of NPA. Yet, using the OCP is the most natural way to introduce $T_e \neq T_i$ in the SCAALP model but it may not be so compatible with the NPA approximation since the OCP is based on a long-range potential that necessitates a neutralizing background. In the NPA approximation, no such background is necessary since we are working with neutral Wigner-Seitz cells. The effective ion-ion potential $\Phi_{eff}(r)$ is by construction short range since it is zero when the radius is larger than two times the Wigner-Seitz radius.

B. Electron-ion relaxation rate

When $T_e \neq T_i$, we have a flow of energy between the electron and ion subsystems until equilibration is reached. In that case, $T_e = T_i = T_{eq}$ where T_{eq} is the equilibration temperature. The time variation of T_e and T_i is usually described by rate equations. Let us establish these equations starting from the total energy density U of the system. Considering only the kinetic energy, U reads [44,45]

$$U = \tfrac{3}{2}N_i k_B T_i + U_e(T_e,T_i), \quad (8)$$

where

$$U_e(T_e,T_i) = \bar{Z}N_i k_B T_e \frac{F_{3/2}(\tilde{\eta})}{F_{1/2}(\tilde{\eta})} \quad (9)$$

and

$$\bar{Z}N_i = \frac{\sqrt{2}(m_e k_B T_e)^{3/2}}{\pi^2\hbar^3} F_{1/2}(\tilde{\eta}). \quad (10)$$

We have introduced the Fermi-Dirac integral [46,47]

$$F_n(\eta) = \int_0^{+\infty} dx \frac{x^n}{1 + e^{x-\eta}} \quad (11)$$

that satisfies

$$F_n'(\eta) = n F_{n-1}(\eta). \quad (12)$$

We make the distinction between $\eta = \mu/k_B Te$ and $\tilde{\eta}$. In practice, they are close to each other. The average ionization $\bar{Z}$ is a function of T_e and T_i, hence U_e and $\tilde{\eta}$. Equation (10) enables us to determine $\tilde{\eta}$ from $\bar{Z}$. We insist on the fact that the effective chemical potential $\tilde{\eta}$ defined by Eq. (10) is precisely the usual reduced chemical potential of an ideal electron gas with density $\bar{Z}N_i$. Ions are classical particles whereas electrons are treated as an ideal Fermi gas that can be degenerate or not.

By definition,

$$\frac{d}{dt}\left(\frac{3}{2}N_i k_B T_i\right) = -g(T_i - T_e) \tag{13}$$

and

$$\frac{d}{dt}U_e(T_e,T_i) = -g(T_e - T_i). \tag{14}$$

This system of equations ensures the conservation of the energy U. The relaxation rate g is usually expressed in $\mathrm{W/m^3\,K}$. It can depend on T_e and T_i. From this factor, one can define a relaxation rate ν_{ie} such that [20,23]

$$g = \tfrac{3}{2}N_i \nu_{ie} k_B. \tag{15}$$

To calculate ν_{ie}, we use the model of Daligault and Dimonte [23], i.e.,

$$\frac{dT_i}{dt} = -\nu_{ie}(T_i - T_e), \tag{16}$$

where the temperature relaxation rate reads

$$\nu_{ie} = -\frac{1}{3\pi^2 m_i}\int_0^{+\infty} dk k^4 \mid \hat{V}_{ei}(k) \mid^2 \frac{\partial \mathrm{Im}\chi_e^0(k,\omega)}{\partial\omega} \mid_{\omega=0}. \tag{17}$$

m_i is the atomic mass of the element. In this expression,

$$\hat{V}_{ei}(k) = \int_0^{R_{WS}} 4\pi r^2 V_{ei}(r)\frac{\sin(kr)}{kr}dr \tag{18}$$

is the Fourier transform of the NPA electron-ion interaction potential $V_{ei}(r)$ and $\chi_e^0(k,\omega)$ is the dynamic density response function of the electron gas. $\chi_e^0(k,\omega)$ is related to the dynamic dielectric function in the random phase approximation (RPA) by

$$\epsilon(k,\omega) = 1 - \frac{4\pi e^2}{k^2}\chi_e^0(k,\omega), \tag{19}$$

where

$$\chi_e^0(k,\omega) = \int \frac{f(\mathbf{p}+\hbar\mathbf{k}/2) - f(\mathbf{p}-\hbar\mathbf{k}/2)}{\hbar\mathbf{k}.\mathbf{p}/m_e - \hbar\omega - i0^+}\frac{2d\mathbf{p}}{(2\pi\hbar)^3}. \tag{20}$$

$f(\mathbf{p})$ is the Fermi-Dirac distribution function

$$f(\mathbf{p}) = \frac{1}{1+\exp\left(\beta_e\frac{p^2}{2m_e} - \tilde{\eta}\right)}. \tag{21}$$

In atomic units, one has [23,37]

$$\frac{\partial \mathrm{Im}\chi_e^0(k,\omega)}{\partial\omega} \mid_{\omega=0} = -\frac{1}{2\pi k}\frac{1}{1+\exp\left(\beta_e\frac{k^2}{8} - \tilde{\eta}\right)}. \tag{22}$$

Screening cuts the divergence at small k and the Fermi-Dirac factor makes the integral convergent at large k. Note that we do not use analytical formulas to describe screening. We simply use the electron-ion potential V_{ei}, derived from $n(r)$, that is used to build the effective electron-ion potential V_{eff} using the pair distribution function [33,34]. This electron-ion potential V_{ei} is naturally screened since we take into account, in a self-consistent way, the bound and free electrons that screen the nuclear charge. This screening is nonlinear and can only be calculated numerically by solving the SCAALP equations. In the present approach, we have neglected electron-electron and electron-ion correlations due to their difficult calculation in dense plasmas. Our approach must be understood to be a first step in the calculation of temperature-relaxation rates in dense plasmas, the next step being the inclusion of electron-electron and electron-ion correlations that can matter [23]. The main advantage of the present approach is that ν_{ie} can be calculated using the RPA approximation and an average-atom model. Doing so, we take into account self-consistently electron degeneracy and screening. We assume weak electron-ion coupling but possibly strong ion-ion coupling. Equation (17) is valid when the ion-excitation spectrum lies well below the electron-excitation spectrum and one uses the fluctuation-dissipation theorem. One can see that the rate of temperature relaxation does not depend on the details of the ionic spectrum of excitations and depends only on the low-frequency properties of the electronic spectrum of fluctuations. Even if the screening can be nonlinear, Eq. (17) is indeed based on the linear-response theory [9]. Note also that expression (17) for ν_{ie} is very similar to the collision frequency calculated using the Born approximation [48] with the exception that ν_{ie} is purely real and that the ion mass appears instead of the electron mass. To derive a rate equation for T_e, one starts from (14). One finds that

$$\frac{\partial U_e}{\partial T_e}\frac{dT_e}{dt} + \frac{\partial U_e}{\partial T_i}\frac{dT_i}{dt} = -g(T_e - T_i). \tag{23}$$

From (9) and (10), one finds that

$$\frac{\partial U_e}{\partial T_e} = \bar{Z}N_i k_B C_e(\tilde{\eta}) + 3N_i k_B T_e \frac{\partial \bar{Z}}{\partial T_e}\frac{F_{1/2}(\tilde{\eta})}{F_{-1/2}(\tilde{\eta})} \tag{24}$$

and

$$\frac{\partial U_e}{\partial T_i} = 3N_i k_B T_e \frac{\partial \bar{Z}}{\partial T_i}\frac{F_{1/2}(\tilde{\eta})}{F_{-1/2}(\tilde{\eta})}, \tag{25}$$

where

$$C_e(\tilde{\eta}) = \frac{5}{2}\frac{F_{3/2}(\tilde{\eta})}{F_{1/2}(\tilde{\eta})} - \frac{9}{2}\frac{F_{1/2}(\tilde{\eta})}{F_{-1/2}(\tilde{\eta})}. \tag{26}$$

These expressions are valid at arbitrary degeneracy. For T_e, one has finally

$$\frac{dT_e}{dt} = -\nu_{ei}(T_e - T_i), \tag{27}$$

where

$$\nu_{ei} = \nu_{ie}\frac{\frac{3}{2} + 3T_e\frac{\partial\bar{Z}}{\partial T_i}\frac{F_{1/2}(\tilde{\eta})}{F_{-1/2}(\tilde{\eta})}}{\bar{Z}C_e(\tilde{\eta}) + 3T_e\frac{\partial\bar{Z}}{\partial T_e}\frac{F_{1/2}(\tilde{\eta})}{F_{-1/2}(\tilde{\eta})}}. \tag{28}$$

When the system is nondegenerate

$$C_e \approx \tfrac{3}{2} \tag{29}$$

and when $\bar{Z}$ is constant, one has the reciprocity relationship [21]

$$\bar{Z}\nu_{ei} \approx \nu_{ie}. \tag{30}$$

In the general case, ν_{ei} is not so simply related to ν_{ie}. The relationship between these two quantities reflects the fact that $\bar{Z}$ depends on both T_e and T_i at fixed mass density. It ensures also that the energy U is conserved during the relaxation process.

The rate equations (16) and (27) are solved starting from initial temperatures T_e^0 and T_i^0 using an explicit scheme. In practice, ν_{ie} and $\bar{Z}$ are calculated with the SCAALP model. We have built a data table of quantities that depend on T_e and T_i at constant mass density. The two-dimensional (2D) Chebychev polynomial interpolation [49] allows ourselves to calculate the quantities of interest for any T_e and T_i inside the data table. In practice, we have tabulated $\bar{Z}$ and ν_{ie}. From the properties of the Chebychev polynomials [49], one can calculate $\frac{\partial \bar{Z}}{\partial T_e}$ and $\frac{\partial \bar{Z}}{\partial T_i}$ from the tabulated values of $\bar{Z}$. The fact that $\bar{Z}$ is usually not constant in dense plasmas complicates the problem. Since our approach conserved the energy U, one can find the equilibration temperature T_{eq} by solving the equation

$$\begin{aligned}&\tfrac{3}{2}N_i k_B T_i^0 + U_e\left(T_e^0, T_i^0\right)\\ &\quad = \tfrac{3}{2}N_i k_B T_{eq} + U_e(T_{eq}, T_{eq}).\end{aligned} \tag{31}$$

From T_{eq}, one can determine the thermodynamic conditions at equilibration and check the accuracy of the numerical scheme used to solve the rates equations (16) and (27).

In the present approach, we have neglected the electron-electron and electron-ion correlations but also the ion-ion correlations in Eq. (31). In order to describe these ion-ion correlations, we characterize the ion subsystem by an effective OCP with an effective parameter Γ_{ii}. The time variation of T_i is now given by

$$\begin{aligned}&\left(1 + \frac{2}{3N_i k_B}\frac{\partial U_{ii}^{ex}}{\partial T_i}\right)\frac{dT_i}{dt} + \left(\frac{2}{3N_i k_B}\frac{\partial U_{ii}^{ex}}{\partial T_e}\right)\frac{dT_e}{dt}\\ &\quad = -\nu_{ie}(T_i - T_e)\end{aligned} \tag{32}$$

whereas (14) is unchanged. Introducing

$$\alpha_{ii} = \frac{2}{3N_i k_B}\frac{\partial U_{ii}^{ex}}{\partial T_i} \tag{33}$$

and

$$\alpha_{ee} = \frac{2}{3N_i k_B}\frac{\partial U_{ii}^{ex}}{\partial T_e} \tag{34}$$

the rate equations including U_{ii}^{ex} read now

$$\frac{dT_i}{dt} = -\nu_{ie}\frac{(T_i - T_e)}{1+\alpha_{ii}}\left(1 + \alpha_{ee}\frac{\frac{3}{2}N_i k_B + \frac{1}{1+\alpha_{ii}}\frac{\partial U_e}{\partial T_i}}{\frac{\partial U_e}{\partial T_e} - \frac{\alpha_{ee}}{1+\alpha_{ii}}\frac{\partial U_e}{\partial T_i}}\right) \tag{35}$$

and

$$\frac{dT_e}{dt} = -\nu_{ie}(T_e - T_i)\frac{\frac{3}{2}N_i k_B + \frac{1}{1+\alpha_{ii}}\frac{\partial U_e}{\partial T_i}}{\frac{\partial U_e}{\partial T_e} - \frac{\alpha_{ee}}{1+\alpha_{ii}}\frac{\partial U_e}{\partial T_i}}. \tag{36}$$

$\frac{\partial U_e}{\partial T_e}$ and $\frac{\partial U_e}{\partial T_i}$ are given by Eqs. (24) and (25). The rate equations (35) and (36) ensure the constancy of $U + U_{ii}^{ex}$. For instance, the equilibration temperature T_{eq} satisfies the equation

$$\begin{aligned}&\tfrac{3}{2}N_i k_B T_i^0 + U_{ii}^{ex}\left(T_e^0, T_i^0\right) + U_e(T_e^0, T_i^0)\\ &\quad = \tfrac{3}{2}N_i k_B T_{eq} + + U_{ii}^{ex}(T_{eq}, T_{eq}) + U_e(T_{eq}, T_{eq})\end{aligned} \tag{37}$$

when we include U_{ii}^{ex} instead of (31). The ion excess energy U_{ii}^{ex} is given by

$$U_{ii}^{ex} = \frac{N_i^2}{2}\int d\mathbf{r}\frac{\bar{Z}^2 e^2}{r}h_{OCP}(r, \Gamma_{ii}), \tag{38}$$

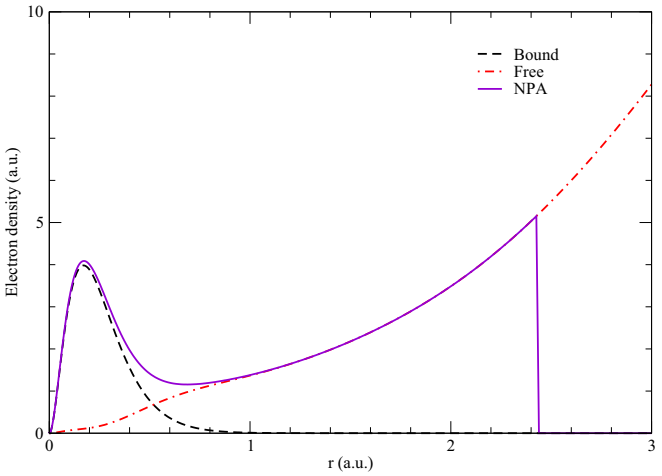

FIG. 1. Electronic densities in a carbon plasma at 2.25 g/cm^3, $T_e = 100$ eV, and $T_i = 10$ eV. We plot the NPA electronic density (solid line) as well as the bound (dashed line) and free (dash-dot line) electronic densities.

where $h_{OCP}(r, \Gamma_{ii})$ is the pair correlation function of the OCP at Γ_{ii}. Here, U_{ii}^{ex} is the excess internal energy per unit volume of the OCP. To see the impact of the correction factor due to ion-ion correlations, we have built a data table of the OCP excess internal energy for Γ_{ii} between 0 and 180 using the Chebychev method [50]. The calculations were done using a hypernetted chain code [51] with the bridge function proposed by Iyetomi *et al.* [52]. The correction factor in (32) is expressed as a function of T_i and Γ_{ii}. The calculation of the derivative with respect to Γ_{ii} is done using the Chebychev method [49] as well as the ones that appear in the calculation of $\partial\Gamma_{ii}/\partial T_i$.

What has been presented in so far in this section does not depend too much on the SCAALP model with $T_e \neq T_i$. We can use an average-atom model with $T_e = T_i$ or even no ionic environment. The rate in Eq. (17) can be computed even in the Thomas-Fermi approximation. Like $\bar{Z}$, the rate will depend

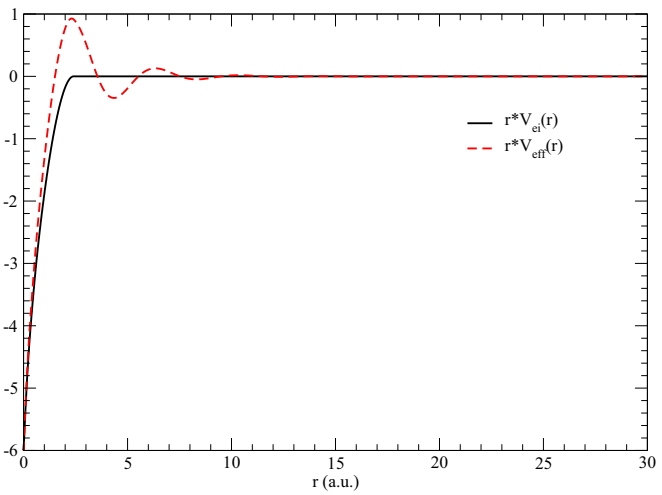

FIG. 2. $r \times V_{ei}(r)$ (solid line) and $r \times V_{eff}(r)$ (dashed line) in a carbon plasma at 2.25 g/cm^3, $T_e = 100$ eV, and $T_i = 10$ eV. $V_{ei}(r)$ and $V_{eff}(r)$ are in atomic units.

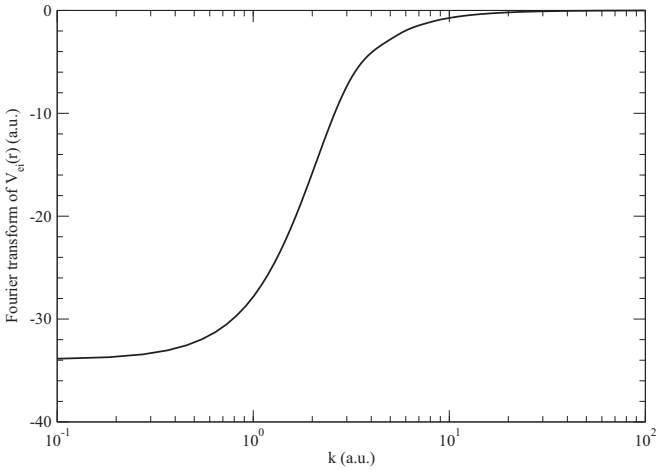

FIG. 3. Fourier transform $\hat{V}_{ei}(k)$ of $V_{ei}(r)$ in a carbon plasma at 2.25 g/cm^3, $T_e = 100$ eV, and $T_i = 10$ eV.

only on T_e. This simplifies Eq. (28) since $\partial \bar{Z}/\partial T_i = 0$. Of course, some physics is missed with such an approach since the rate equations (16) and (27) are less coupled. This may impact the relaxation to equilibrium.

III. NUMERICAL APPLICATIONS

As a first application we consider a carbon plasma at solid density $\rho = 2.25$ g/cm^3 with $T_e = 100$ eV and $T_i = 10$ eV. We find that $\bar{Z} = 4.17$. We plot in Fig. 1 the NPA electronic density, which is truncated in $R_{WS} = 2.43$ a.u., and the bound and free components. The bump near $r = 0.18$ a.u. is related to the $1s$ orbital. We plot in Fig. 2 the two potentials $V_{ei}(r)$ and $V_{eff}(r)$. As expected, $V_{ei}(r) = 0$ when $r > R_{WS}$. One can see in this figure the effect of the environment taken into account in $V_{eff}(r)$. The more structured the pair correlation function, the more $V_{eff}(r)$ oscillates around zero. We plot in Fig. 3 the Fourier transform $\hat{V}_{ei}(k)$ of $V_{ei}(r)$. One can see that $\hat{V}_{ei}(k)$ does not diverge as $1/k^2$ at small wave number k due to screening. For the cases considered in this work, the average ionization depends weakly on T_i at fixed T_e.

As a second application, we consider a hydrogen plasma. We plot in Table I the plasmas parameters considered [20]. We give in Table II the relaxation rate g in W/m^3 K for the cases shown in Table I. We compare the SCAALP calculations with another average-atom model [53] (AA), Brown-Preston-Singleton [11] (BPS), and Landau-Spitzer [4,5] (LS). SCAALP and AA cases use Eqs. (17) and (15). One can see that when the density is increasing, the relaxation rate g is smaller than the other cases. This means that the relaxation

TABLE I. Hydrogen plasma configurations [20]. The ion density N_i is in cm^{-3} and the electron and ion temperatures are in eV.

Symbol	A	B	C	D
N_i	2.4×10^{22}	2.68×10^{23}	7.59×10^{23}	2.4×10^{25}
T_e	80	400	800	8000
T_i	100	500	1000	10000

TABLE II. Relaxation rate g in W/m^3 K for the cases considered in Table I. SCAALP calculations (SCAALP) are compared to another average-atom model [53] (AA), Brown-Preston-Singleton [11] (BPS), and Landau-Spitzer [4,5] (LS). AA, BPS, and LS data are taken from Ref. [20].

	$A \times 10^{17}$	$B \times 10^{18}$	$C \times 10^{18}$	$D \times 10^{20}$
MD	1.03	0.98	4.06	
SCAALP	0.87	0.97	2.74	0.87
AA	0.88	1.40	4.62	1.74
BPS	1.53	1.94	5.79	2.14
LS	0.90	1.24	3.81	1.51

is longer with the SCAALP model. Compared to AA, the difference comes from the calculation of the Fourier transform of the electron-ion interaction potential $V_{ei}(r)$. Screening can be important in the calculation of the relaxation rate. One may also question the use of an average-atom model to describe a hydrogen plasma. In principle, the average-atom model is more sound to treat many-electron atoms in which the statistical approximation really makes sense. As an illustration, we plot in Fig. 4 the relaxation of T_e and T_i starting from $T_e^0 = 30$ eV and $T_i^0 = 60$ eV for $N_i = 10^{22}$ cm^{-3} (case D of Ref. [19]). Molecular dynamics simulations (MD) [28] are compared to SCAALP calculations (SCAALP) and the Gericke-Murillo-Schlanges model (GMS) [10]. The MD simulations were carried out treating the electrons and ions classically and using semiclassical potentials as in MD simulations of Ref. [19]. No recombination or ionization processes were taken into account, as in Refs. [54,55]. Compared to MD, SCAALP (GMS) relaxation is longer (shorter). Since the average ionization is slightly different from 1, the equilibration temperature for the SCAALP case is different from 45 eV. At the equilibration estimated reached after 20 ps, $T_{eq} = 44.96$ eV, $\bar{Z}_{eq} = 0.97$, and $g_{eq} = 3.63 \times 10^{16}$ W/m^3 K. The fact that $\bar{Z} \neq 1$ during the relaxation process makes the curves not symmetric with

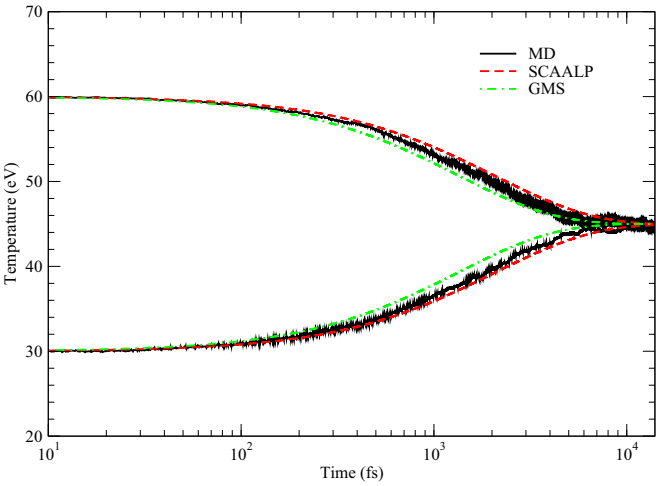

FIG. 4. Relaxation of T_e and T_i starting from $T_e^0 = 30$ eV and $T_i^0 = 60$ eV for a hydrogen plasma at $N_i = 10^{22}$ cm^{-3}. Molecular dynamics simulations (MD) are compared to SCAALP calculations (SCAALP) and the model of Gericke-Murillo-Schlanges (GMS) [10].

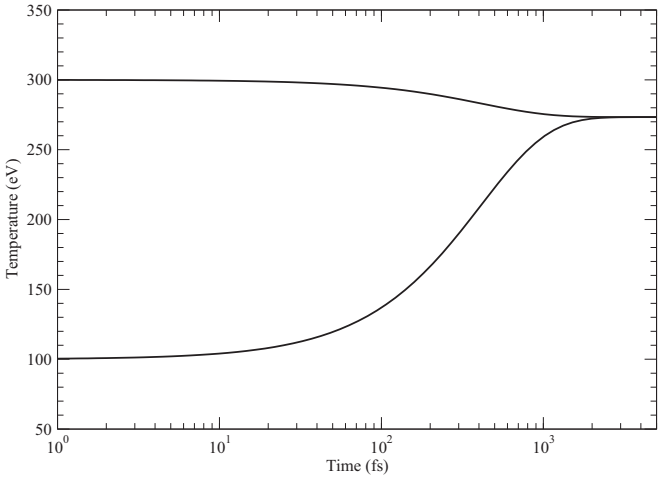

FIG. 5. Relaxation of T_e and T_i starting from $T_e^0 = 300$ eV and $T_i^0 = 100$ eV for a carbon plasma at $\rho = 2.25$ g/cm^3 using the SCAALP model.

respect to the line $T = T_{eq}$. In the present case, the fact that $\bar{Z} \neq 1$ has a negligible impact on the relaxation time. Knowing the approximations involved in our approach, one can say that the agreement with MD simulations is good. In the present case, note that GMS is in better agreement with MD data than BPS [11] or LS [4,5].

As a third application, we consider solid-density carbon plasmas. As an example, we consider the relaxation starting from $T_e^0 = 300$ eV and $T_i^0 = 100$ eV using the SCAALP model. In Fig. 5, we plot the temperature relaxation as a function of time. Due to Eq. (28), we can see that the relaxation is asymmetric, the ion temperature relaxing more than the electron temperature. At equilibrium, $T_{eq} = 273.3$ eV, $\bar{Z}_{eq} = 5.52$, and $g_{eq} = 5.25 \times 10^{18}$ W/m^3 K. We plot in Fig. 6 the relaxation of the average ionization $\bar{Z}$ as a function of time. Since this quantity depends more on T_e than on T_i and since T_e does not change too much during the relaxation, $\bar{Z}$ stays close to 5.5–5.6. We give in Tables III and IV the equilibration

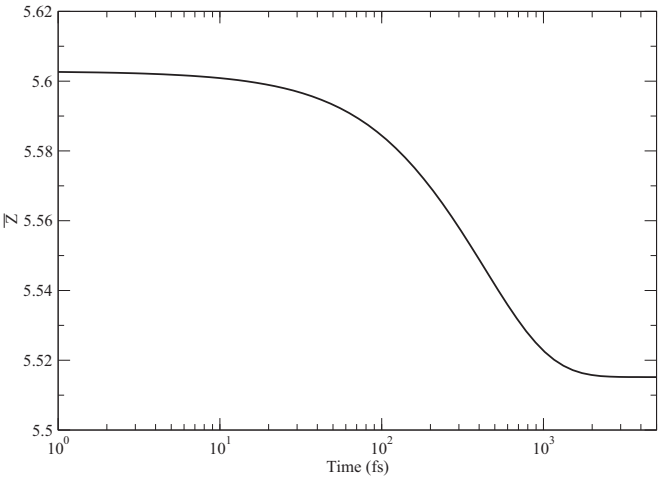

FIG. 6. Relaxation of $\bar{Z}$ starting from $T_e^0 = 300$ eV and $T_i^0 = 100$ eV for a carbon plasma at $\rho = 2.25$ g/cm^3 using the SCAALP model.

TABLE III. Equilibration temperature T_{eq} as a function of T_e^0 (line) and T_i^0 (column) in a carbon plasma at $\rho = 2.25$ g/cm^3 using the SCAALP model. Temperatures are in eV.

	10	30	50	70	100	300	500	700	1000
10		14.63	19.13	23.53	30.02	68.72	100.1	128.4	169.0
30	25.61		34.12	38.20	44.16	79.46	109.6	137.2	177.7
50	41.96	46.12		53.66	59.33	91.40	120.2	147.5	187.9
70	59.39	63.27	66.58		74.80	104.7	132.5	159.4	199.8
100	86.25	89.75	92.71	95.83		127.5	154.3	181.1	221.6
300	260.9	264.0	266.8	269.4	273.3		327.3	355.0	396.9
500	432.6	435.7	438.4	441.2	445.1	472.3		527.9	570.2
700	604.3	607.2	609.9	612.5	616.7	644.0	671.9		742.3
1000	861.3	864.4	867.1	870.0	873.9	901.5	929.5	957.6	

temperature T_{eq} and average ionization at equilibration $\bar{Z}_{eq}$ starting from various T_e^0 and T_i^0. One can see that we need a relatively large difference between T_e^0 and T_i^0 in order for T_{eq} to deviate significantly from T_e^0. One can note also that the results are smooth functions of T_e^0 and T_i^0. In could be interesting to compare the results presented in Tables III and IV with classical molecular dynamics simulations of dense plasmas [54,55]. Note finally that the system becomes coupled when T_i is small. This indicates that we may reach the limit of validity of the present approach at low T_i since we neglect the Coulomb contributions between ion-ion, ion-electron, and electron-electron. These contributions can be important in the warm dense matter regime, especially the ion-ion one when Γ_{ii} changes noticeably during a relaxation [12]. As an example, let us take the case $T_e^0 = 100$ eV and $T_i^0 = 10$ eV. In Fig. 7, we plot the evolution of Γ_{ii} during the relaxation. Γ_{ii} changes between 19.5 and 2.0, meaning that the ion-ion correlations can play a role. To see this, we plot in Fig. 8 the relaxation of T_e and T_i without the correction (wo) due to the ion excess energy U_{ii}^{ex} and with this correction (wi). As found previously by Gericke [12], the ions heat much slower at the beginning of the relaxation if the ion correlations are taken into account and the electron temperature decreases much faster. Note that the overall relaxation is slower and the equilibration temperature T_{eq} is also affected. Without the correction, we find $T_{eq} = 86.25$ eV whereas with the correction, we find $T_{eq} = 80.84$ eV. The full calculation reaches a lower temperature than the ideal one since U_{ii}^{ex} becomes less negative during the relaxation [12].

TABLE IV. Average ionization at equilibration $\bar{Z}_{eq}$ as a function of T_e^0 (line) and T_i^0 (column) in a carbon plasma at $\rho = 2.25$ g/cm^3 using the SCAALP model. Temperatures are in eV.

	10	30	50	70	100	300	500	700	1000
10		2.61	2.76	2.87	3.01	3.64	4.17	4.59	5.02
30	2.92		3.09	3.15	3.25	3.84	4.32	4.70	5.08
50	3.21	3.27		3.38	3.47	4.04	4.47	4.81	5.16
70	3.47	3.54	3.60		3.75	4.24	4.64	4.93	5.23
100	3.95	4.00	4.06	4.11		4.57	4.88	5.11	5.34
300	5.48	5.49	5.50	5.51	5.52		5.62	5.66	5.71
500	5.74	5.74	5.74	5.75	5.75	5.77		5.80	5.82
700	5.83	5.83	5.83	5.83	5.83	5.84	5.85		5.87
1000	5.89	5.89	5.89	5.89	5.89	5.90	5.90	5.90	

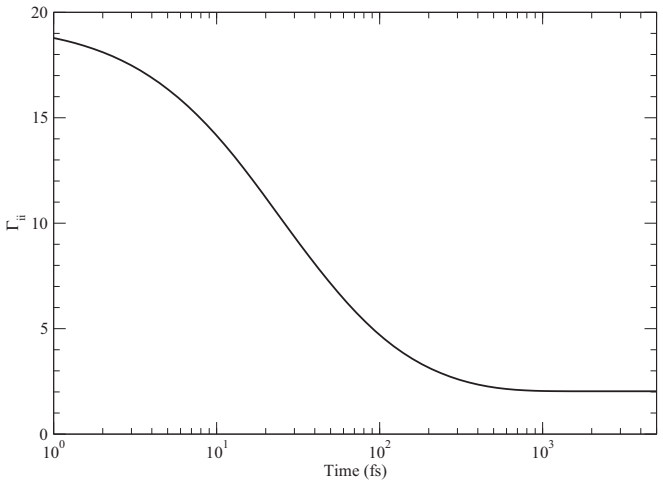

FIG. 7. Relaxation of Γ_{ii} starting from $T_e^0 = 100$ eV and $T_i^0 = 10$ eV for a carbon plasma at $\rho = 2.25$ g/cm^3 using the SCAALP model.

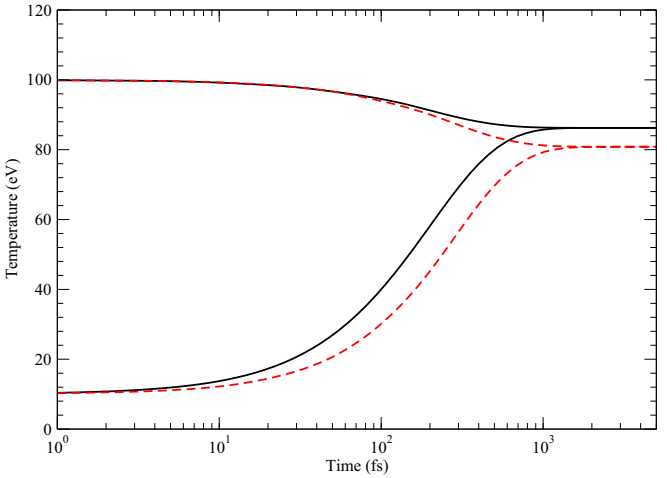

FIG. 8. Relaxation of T_e and T_i starting from $T_e^0 = 100$ eV and $T_i^0 = 10$ eV for a carbon plasma at $\rho = 2.25$ g/cm^3 using the SCAALP model without the correction (solid line) due to the ion excess energy and with this correction (dashed line).

These results were obtained for $T_e^0 > T_i^0$. When $T_i^0 > T_e^0$, we find the opposite effect since the initial ion system is initially less coupled than at equilibration, i.e., U_{ii}^{ex} becomes more negative during the relaxation. As an illustration, if $T_e^0 = 10$ eV and $T_i^0 = 100$ eV, we find that $T_{eq} = 30.02$ eV without the OCP correction but $T_{eq} = 37.69$ eV with this OCP correction. Of course, the present approach is an approximation since we consider an OCP system and we neglect screening but it gives a relative good overview of the physics involved. The complete treatment of the relaxation that takes into account in a self-consistent way the ion-ion (beyond the OCP approximation), ion-electron, and electron-electron correlations to go beyond the ideal gas approximation is still to be developed.

IV. CONCLUSION

We have presented a model to calculate rates of temperature-relaxation in dense plasmas using an average-atom model. An approximate way has been described to consider the case where the electron and ion temperatures T_e and T_i are different directly inside the average-atom model. This enriches the model since the rates and the average ionization depend on T_e and T_i but complicates the resolution of the rate equations. Comparison with molecular dynamics simulations for a hydrogen plasma have shown that this approach makes sense. We have also studied the role of ionization along the temperature relaxation for solid-density carbon plasmas. We have gone beyond the usual treatment of the kinetic energy balance in such kind of study by considering the role of ion-ion correlations using the OCP approximation. The effect is to lower the equilibration temperature compared to the case when we consider only the kinetic energy balance when the initial electron temperature T_e^0 is greater than the initial ion temperature T_i^0. We have the opposite effect when T_i^0 is greater than T_e^0. The next step consists of taking into account from first principles electron-electron, electron-ion, and ion-ion correlations beyond the OCP approximation as well as treating mixtures.

[1] S. Atzeni and J. Meyer-ter-Vehn, *The Physics of Inertial Fusion: Beam Plasma Interaction, Hydrodynamics, Hot Dense Matter* (Clarendon Press, Oxford, 2004).
[2] J. R. Rygg, J. A. Frenje, C. K. Li, F. H. Séguin, R. D. Petrasso, D. D. Meyerhofer, and C. Stoeckl, Phys. Rev. E **80**, 026403 (2009).
[3] B. Xu and S. X. Hu, Phys. Rev. E **84**, 016408 (2011).
[4] L. D. Landau, Phys. Z. Sowjetunion **10**, 154 (1936); Zh. Eksp. Teor. Fiz. **7**, 203 (1937).
[5] L. Spitzer Jr., *Physics of Fully Ionized Gases*, 2nd ed. (Interscience, New York, 1962).
[6] T. Kihara and O. Aono, J. Phys. Soc. Jpn. **18**, 837 (1963).
[7] M. W. C. Dharma-wardana and F. Perrot, Phys. Rev. E **58**, 3705 (1998).
[8] M. W. C. Dharma-wardana, Phys. Rev. E **64**, 035401(R) (2001).
[9] G. Hazak, Z. Zinamon, Y. Rosenfeld, and M. W. C. Dharma-wardana, Phys. Rev. E **64**, 066411 (2001).
[10] D. O. Gericke, M. S. Murillo, and M. Schlanges, Phys. Rev. E **65**, 036418 (2002).
[11] L. S. Brown, D. L. Preston, and R. L. Singleton Jr., Phys. Rep. **410**, 237 (2005).
[12] D. O. Gericke, J. Phys.: Conf. Ser. **11**, 111 (2005).
[13] L. S. Brown and R. L. Singleton Jr., Phys. Rev. E **76**, 066404 (2007).
[14] J. Daligault and D. Mozyrsky, Phys. Rev. E **75**, 026402 (2007).
[15] J. Daligault and D. Mozyrsky, High Energy Density Phys. **4**, 58 (2008).
[16] G. Gregori and D. O. Gericke, Europhys. Lett. **83**, 15002 (2008).
[17] M. S. Murillo and M. W. C. Dharma-wardana, Phys. Rev. Lett. **100**, 205005 (2008).

[18] M. W. C. Dharma-wardana, Phys. Rev. Lett. **101**, 035002 (2008).
[19] J. N. Glosli, F. R. Graziani, R. M. More, M. S. Murillo, F. H. Streitz, M. P. Surh, L. X. Benedict, S. Hau-Riege, A. B. Langdon, and R. A. London, Phys. Rev. E **78**, 025401(R) (2008).
[20] B. Jeon, M. Foster, J. Colgan, G. Csanak, J. D. Kress, L. A. Collins, and N. Grønbech-Jensen, Phys. Rev. E **78**, 036403 (2008).
[21] G. Dimonte and J. Daligault, Phys. Rev. Lett. **101**, 135001 (2008).
[22] L. S. Brown and R. L. Singleton Jr., Phys. Rev. E **79**, 066407 (2009).
[23] J. Daligault and G. Dimonte, Phys. Rev. E **79**, 056403 (2009).
[24] J. Vorberger and D. O. Gericke, Phys. Plasmas **16**, 082702 (2009).
[25] J. Vorberger, D. O. Gericke, T. Bornath, and M. Schlanges, J. Phys.: Conf. Ser. **220**, 012002 (2010).
[26] J. Vorberger, D. O. Gericke, T. Bornath, and M. Schlanges, Phys. Rev. E **81**, 046404 (2010).
[27] L. X. Benedict, M. P. Surh, J. I. Castor, S. A. Khairallah, H. D. Whitley, D. F. Richards, J. N. Glosli, M. S. Murillo, C. R. Scullard, P. E. Grabowski, D. Michta, and F. R. Graziani, Phys. Rev. E **86**, 046406 (2012).
[28] C. Blancard, J. Clérouin, and G. Faussurier, High Energy Density Phys. **9**, 247 (2013).
[29] D. A. Chapman, J. Vorberger, and D. O. Gericke, Phys. Rev. E **88**, 013102 (2013).
[30] J. Vorberger and D. O. Gericke, High Energy Density Phys. **10**, 1 (2014).
[31] Q. Ma, J. Dai, D. Kang, Z. Zhao, J. Yuan, and X. Zhao, High Energy Density Phys. **13**, 34 (2014).
[32] Z. G. Fu, Z. Wang, D. F. Li, W. Kang, and P. Zhang, Phys. Rev. E **92**, 033103 (2015).
[33] C. Blancard and G. Faussurier, Phys. Rev. E **69**, 016409 (2004).
[34] G. Faussurier, C. Blancard, P. Cossé, and P. Renaudin, Phys. Plasmas **17**, 052707 (2010).
[35] H. Iyetomi and S. Ichimaru, Phys. Rev. A **34**, 433 (1986).
[36] J. P. Hansen and I. R. McDonald, *Theory of Simple Liquids*, 2nd ed. (Academic, London, 1986).
[37] W. R. Johnson, J. Nilsen, and K. T. Cheng, Phys. Rev. E **86**, 036410 (2012).
[38] R. M. More, Adv. At. Mol. Phys. **21**, 305 (1985).
[39] R. M. More, K. H. Warren, D. A. Young, and G. B. Zimmerman, Phys. Fluids **31**, 3059 (1988).
[40] C. Blancard, P. Cossé, and G. Faussurier, Astrophys. J. **745**, 10 (2012).
[41] A. N. Souza, D. J. Perkins, C. E. Starrett, D. Saumon, and S. B. Hansen, Phys. Rev. E **89**, 023108 (2014).
[42] T. Blenski and K. Ishikawa, Phys. Rev. E **51**, 4869 (1995).
[43] D. B. Boercker and R. M. More, Phys. Rev. A **33**, 1859 (1986).
[44] L. Landau and E. Lifchitz, *Physique Statistique* (Editions Mir, Moscow, 1984).
[45] R. P. Feynman, *Statistical Mechanics - A Set of Lectures* (Addison-Wesley, New York, 1990).
[46] J. S. Blakemore, Solid State Electron. **25**, 1067 (1982).
[47] M. Goano, Solid State Electron. **36**, 217 (1993).
[48] R. Thiele, T. Bornath, C. Fortmann, A. Höll, R. Redmer, H. Reinholz, G. Röpke, A. Wierling, S. H. Glenzer, and G. Gregori, Phys. Rev. E **78**, 026411 (2008).
[49] W. H. Press, S. A. Teukolski, W. T. Vetterling, and B. P. Flannery, *Numerical Recipes in Fortran: The Art of Scientific Computing*, 2nd ed. (Cambridge University Press, New York, 1992).
[50] G. Faussurier and M. S. Murillo, Phys. Rev. E **67**, 046404 (2003).
[51] G. Faussurier, Phys. Rev. E **69**, 066402 (2004).
[52] H. Iyetomi, S. Ogata, and S. Ichimaru, Phys. Rev. A **46**, 1051 (1992).
[53] G. Csanak and W. Daughton, J. Quant. Spectrosc. Radiat. Transfer **83**, 83 (2004).
[54] F. R. Graziani *et al.*, High Energy Density Phys. **8**, 105 (2012).
[55] S. P. Hau-Riege, J. Weisheit, J. I. Castor, R. A. London, H. Scott, and D. F. Richards, New J. Phys. **15**, 015011 (2013).